

Zeolite membranes – The importance of support analysis

Kapteijn, Freek; Wang, Xuerui

DOI

[10.1002/cite.202100136](https://doi.org/10.1002/cite.202100136)

Publication date

2022

Document Version

Final published version

Published in

Chemie-Ingenieur-Technik

Citation (APA)

Kapteijn, F., & Wang, X. (2022). Zeolite membranes – The importance of support analysis. *Chemie-Ingenieur-Technik*, 94(1-2), 23-30. <https://doi.org/10.1002/cite.202100136>

Important note

To cite this publication, please use the final published version (if applicable). Please check the document version above.

Copyright

Other than for strictly personal use, it is not permitted to download, forward or distribute the text or part of it, without the consent of the author(s) and/or copyright holder(s), unless the work is under an open content license such as Creative Commons.


Takedown policy

Please contact us and provide details if you believe this document breaches copyrights. We will remove access to the work immediately and investigate your claim.

Zeolite Membranes – The Importance of Support Analysis

Freek Kapteijn^{1,*} and Xuerui Wang²

DOI: 10.1002/cite.202100136

 This is an open access article under the terms of the Creative Commons Attribution-NonCommercial License, which permits use, distribution and reproduction in any medium, provided the original work is properly cited and is not used for commercial purposes.

Dedicated to Prof. Dr. rer. nat. Jürgen Caro on the occasion of his 70th birthday

Zeolite membranes are highly attractive in energy efficient, selective separation technologies. Their high selectivity originates from selective adsorption, diffusion and even molecular sieving. High flux zeolite membranes ($> 1 \text{ mol s}^{-1} \text{ m}^{-2}$) with a sub-micrometer thickness are mechanically stabilized by a porous, often multilayer, support. Transport mechanisms in zeolite layer and support, however, are counteracting regarding selectivity, and a support may also act as a flux resistance. Several examples are analyzed quantifying the impact of the support on the observed performance, showing the effect of layer thickness, orientation of the asymmetric membrane and operational conditions, resulting in recommendations for the configuration of zeolite membrane modules.

Keywords: Gas separation, High-flux membrane, Pervaporation, Support, Zeolite membrane

Received: July 09, 2021; *revised:* November 25, 2021; *accepted:* December 12, 2021

1 Introduction

Zeolite membranes have been identified as promising materials for separation of gas or liquid mixtures that otherwise require energy intensive operations. Prof. Juergen Caro, together with Manfred Noack, is among the pioneers in this field and have contributed a lot to the development and application of this type of membranes [1–5]. In spite of the promising separation principles, potential of molecular sieving, application on a large scale is still limited. This is mainly due to the challenging large scale and cost-effective reproducible manufacture of these membranes, although a gradual penetration of zeolite membrane applications is visible [1, 6–10]. The first application was in the separation of water-ethanol mixtures and breaking its azeotrope by zeolite A membrane, later followed by dehydration of other organics over other zeolite membranes with the MFI, FAU, DDR, CHA structures or derivatives [5, 11–15]. Improved synthesis techniques led to this broader variation in zeotypes, but also to increased fluxes through these membranes [16–20]. As a result, the influence of the support on the membrane performance becomes more prominent, both in terms of permeance and of selectivity, a subject that we touched upon in earlier publications [21–5].

In this contribution the various observed aspects of the influence or impact of the support on the performance of the zeolite membrane as a whole are presented. The examples in this contribution show the importance of taking the support characteristics into consideration for a specific application, and some recommendations are provided for the design of the zeolite-based membranes.

2 Theoretical Aspects

Depending on the zeolite structure (pore or window openings formed by 12, 10, or 8 oxygen anions) and composition (hydrophilic or hydrophobic character) and the size or shape and polarity of the molecules zeolite membranes separate gas or liquid mixtures based on the relative extent of competitive (ad)sorption and diffusion contributions. The smaller the pore or window size going from 12 to 8 membered-ring zeolites, the more difficult the diffusion through the zeolite, so the bulkier the molecule the more it will be rejected, with as ultimate limit molecular sieving (Fig. 1) [26, 27]. The latter assumes a rigid zeolite structure, which is true to a large extent, although some flexibility effects have been reported in separation [28–31].

Transport through the zeolite layer can be described by the consecutive phenomena of sorption-diffusion-desorption. Usually, the diffusion is assumed to be the slow step and sorption and desorption infinitely fast, equilibrated. Surface or intracrystalline barriers are not considered here,

¹Prof. Dr. Freek Kapteijn
f.kapteijn@tudelft.nl

Delft University of Technology, Catalysis Engineering – Chemical Engineering Department, Van der Maasweg 9, 2629 HZ Delft, The Netherlands.

²Prof. Dr. Xuerui Wang

Nanjing Tech University, State Key Laboratory of Materials-Oriented Chemical Engineering, College of Chemical Engineering, Jiangsu National Synergetic Innovation Center for Advanced Materials, No. 30 Puzhu South Road, Nanjing 211816, China.

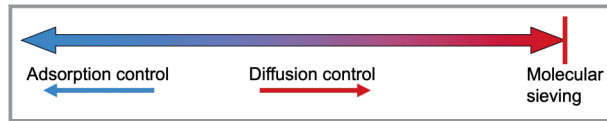


Figure 1. Separation mechanisms of zeolite membranes ranging from selective sorption, diffusion to molecular sieving, depending on the affinity and pore/window size of the zeolite type.

these will result in additional transport resistances and require more elaborate modeling relations [32–35].

Under the abovementioned assumptions, Langmuir adsorption and application of the Generalized Maxwell-Stefan (GMS) approach [36–38], the single component permeation flux through a silicalite-1 membrane could be described by Eq. (1).

$$N_i = -q_i^{\text{sat}} \rho \frac{D_i}{1 - \theta_i} \nabla \theta_i = q_i^{\text{sat}} \rho D_i \nabla \ln(1 - \theta_i) \quad (1)$$

Substitution of the Langmuir isotherm gives:

$$N_i = q_i^{\text{sat}} \rho D_i \frac{\ln\left(\frac{1+K_i p_{i,0}}{1+K_i p_{i,\delta}}\right)}{\delta} \quad (2)$$

with for the low loading regime

$$N_i = -q_i^{\text{sat}} \rho D_i K_i \frac{\Delta p_i}{\delta} \quad (3)$$

The ideal selectivity based on pure single component permeation then reads

$$S_{12}^{\text{ideal}} = \left(\frac{D_1}{D_2}\right) \left(\frac{q_1^{\text{sat}} K_1}{q_2^{\text{sat}} K_2}\right) = S_{12}^{\text{diff}} S_{12}^{\text{ads}} \quad (4)$$

At high loadings (saturation) the flux can be approximated by

$$N_i = -q_i^{\text{sat}} \rho D_i \frac{\Delta \ln p_i}{\delta} \quad (5)$$

and only the zeolitic diffusivity is controlling. In such cases, however, it becomes questionable if the assumptions still hold. In such situations the effect of the support becomes important to estimate the real partial pressures at the zeolite-support interface for a proper transport modeling. These relations clearly show the influence of both the adsorption and diffusivity on the flux.

For binary mixtures the extended Langmuir adsorption isotherm

$$q_i = q_i^{\text{sat}} \frac{K_i p_i}{1 + \sum K_j p_j} \quad (6)$$

and the GMS approach yields for the selectivity [37]

$$S_{12} = \frac{N_1 y_2}{N_2 y_1} = \frac{q_1^{\text{sat}} D_1 \left[\left\{ \Gamma_{11} + \theta_1 \frac{D_1}{D_{12}} (\Gamma_{11} + \Gamma_{21}) \right\} \nabla \theta_1 + \left\{ \Gamma_{12} + \theta_1 \frac{D_1}{D_{12}} (\Gamma_{12} + \Gamma_{22}) \right\} \nabla \theta_2 \right] y_2}{q_2^{\text{sat}} D_2 \left[\left\{ \Gamma_{22} + \theta_2 \frac{D_1}{D_{12}} (\Gamma_{22} + \Gamma_{12}) \right\} \nabla \theta_2 + \left\{ \Gamma_{21} + \theta_2 \frac{D_1}{D_{12}} (\Gamma_{21} + \Gamma_{11}) \right\} \nabla \theta_1 \right] y_1} \quad (7)$$

which simplifies for low loadings to

$$\lim_{\theta_1, \theta_2 \rightarrow 0} S_{12} = \left(\frac{D_1}{D_2}\right) \left(\frac{q_1^{\text{sat}} K_1 p_1 y_2}{q_2^{\text{sat}} K_2 p_2 y_1}\right) = S_{12}^{\text{diff}} S_{12}^{\text{ads}} \quad (8)$$

which is the same expression as for the ideal selectivity. With increasing loading the stronger adsorbing component will hinder the usually faster component and the selectivity is usually in favor of the former. Due to this competitive adsorption, the mixture selectivity then clearly differs from the ideal (single component) selectivity.

For high loadings and where component 1 is the stronger adsorbing and slower diffusing one the mixture selectivity becomes

$$\lim_{\theta_1 + \theta_2 \rightarrow 1} S_{12} = \left(\frac{q_1^{\text{sat}} \theta_1 y_2}{q_2^{\text{sat}} \theta_2 y_1}\right) \frac{1 + \frac{D_{12}}{D_2}}{2} = S_{12}^{\text{ads}} \frac{1 + \frac{D_{12}}{D_2}}{2} \quad (9)$$

For this fictitious mixture D_{12} is much smaller than D_2 so the maximum achievable selectivity is close to $1/2 S_{12}^{\text{ads}}$. This illustrates that for an equimolar mixture of this system the membrane separation selectivity is lower than the adsorption selectivity.

This modeling result clearly indicates that mixture selectivity depends on the competitive adsorption and diffusion properties of the individual components in the mixture. The extended Langmuir isotherm is only an approximation for competitive adsorption (unequal saturation loadings) and the IAS Theory yields a better approximation [38], but the simplification still serves here as a good illustration. Often a weaker adsorbing component diffuses faster, so the net selectivity result is not a priori predicted, and experimental conditions (partial pressures and temperature) affect this strongly, see below [22].

Because of the thickness in the order of only (sub)micrometers, the zeolite membrane layer is generally prepared on a thicker (~mm) micro/macro-porous support, mechanically stabilizing the thin, fragile zeolite layer. This support, usually in the order of 1–3 mm thickness, can have uniform porosity and pore size, or a gradient in pore size, or consisting of two or more layers of different thickness and pore sizes [25, 39]. Usually, the zeolite layer of the asymmetric membrane faces the feed side.

Depending on the applied conditions transport through the support will be mainly governed by Knudsen or molecular diffusion and viscous flow, and possibly a combination of these mechanisms. Evacuating the permeate side will result in Knudsen transport

$$N_{Kn,i} = -\frac{1}{RT} D_{Kn,i}^{eff} \nabla p_i \quad (10)$$

with

$$D_{Kn,i}^{eff} = \frac{\varepsilon_{sup}}{\tau_{sup}} \frac{d_o}{3} \sqrt{\left(\frac{8RT}{\pi M_i}\right)} \quad (11)$$

while using a sweep gas can lead to molecular diffusion through the nearly stagnant gas in the support. This can be described by the GMS relations for porous media ('Dusty gas model' [40]). For a single permeating component diffusing in helium through the support the flux reads

$$N_{mol,i} = -\frac{1}{RT} \left(\frac{\varepsilon_{sup}}{\tau_{sup}}\right) D_{iHe} \nabla p_i \quad (12)$$

with

$$D_{AB} = \frac{10^{-7} T^{1.75} \left(\frac{1}{M_A} + \frac{1}{M_B}\right)^{1/2}}{p_{tot} \left(\left(\sum_A v_a\right)^{1/3} + \left(\sum_B v_a\right)^{1/3} \right)^2} \quad (13)$$

Higher fluxes through the membrane may even result in a viscous flow contribution.

$$N_{vis,i} = -\left(\frac{\bar{p}_i}{RT}\right) \frac{B_0^{eff}}{\eta} \nabla p_{tot} \quad (14)$$

with

$$B_0^{eff} = \frac{\varepsilon_{sup}}{\tau_{sup}} \frac{d_o^2}{32} \quad (15)$$

It is noted here that viscous flow and molecular diffusion will not yield separation selectivity, only Knudsen transport results in a separation selectivity inversely proportional to the square root of the molar masses of the diffusing components

$$S_{12}^{Kn} = \sqrt{\frac{M_2}{M_1}} \quad (16)$$

For a multilayer support the layer resistance for Knudsen transport is proportional to the ratio of layer thickness δ and pore size d_o , assuming identical porosity and tortuosity of the layers. As illustration serves the data of De Bruijn et al. for a four-layer support with structural parameters given in Tab. 1 [25].

Under evacuation conditions often the major resistance of such a support is usually formed by the thickest, coarsest base layer. However, for higher membrane fluxes and higher pressures the viscous flow becomes an important contribution, lowering the pressure drop over the support. In those cases the finer top layer(s) should also be considered (see Sect. 3.4).

Table 1. Structural parameters of a four-layer support and relative Knudsen resistance [25].

Layer #		Thickness δ	Pore size d_o	Porosity ε	% Knudsen Resistance
1	γ -Al ₂ O ₃	3 μ m	4 nm	0.60	11
2	α -Al ₂ O ₃	40 μ m	0.18 μ m	0.35	6
3	α -Al ₂ O ₃	40 μ m	0.28 μ m	0.35	4
4	α -Al ₂ O ₃	3 mm	1 μ m	0.35	79

A full analysis of mixture permeation over a multilayer membrane, based on the Dusty gas model, considering Knudsen and molecular diffusion and viscous flow, can be found elsewhere [39].

Under Knudsen conditions (low pressure, small pores) light molecules diffuse faster in mixtures, whereas for zeolite membranes the opposite was found (see below). Therefore, the selective zeolite layer and the support have counteracting separation characteristics, as will be demonstrated below. In the case intrinsic diffusivity parameters are to be determined for the selective layer [41], the influence of the support should be negligibly small or included in the modeling analysis.

Often the permeance of a membrane ($\Pi_i = N_i/\Delta p_i$) is used as an indicator of the controlling process in the permeation, as the different transport mechanisms show a different pressure dependency, cf. Eqs. (2), (10), and (14). Once experimentally the component fluxes (and selectivity) through the composite zeolite membrane have been determined, the relations above can be used to determine the partial pressures at the zeolite-support interface and quantify the contribution of the support in the pressure drop over the whole membrane, i.e., determine the support resistance in terms of the pressure drops over the different layers. This is schematically explained in Fig. 2.

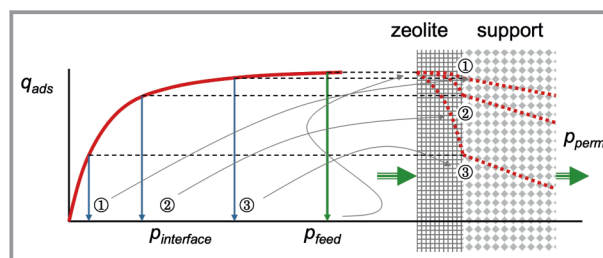


Figure 2. Schematic illustration of concentration gradients in a zeolite membrane at different permeate pressures which determine the local zeolite loading at the zeolite-support interface.

This allows then to determine the real pressure gradient and calculate the correct permeance over the zeolite layer, which is essential in modeling studies to describe the transport through this layer. This is illustrated for the room temperature unary permeation of CO₂, H₂, and N₂ through an

alumina supported SSZ-13 membrane at different feed pressures and atmospheric permeate pressure, no sweep gas was used (Fig. 3). The structural parameters of the support were determined independently without zeolite layer. In this case the main support correction was due to Knudsen transport. For this support this correction becomes significant for permeances above $5 \times 10^{-7} \text{ mol m}^{-2} \text{ s}^{-1} \text{ Pa}^{-1}$.

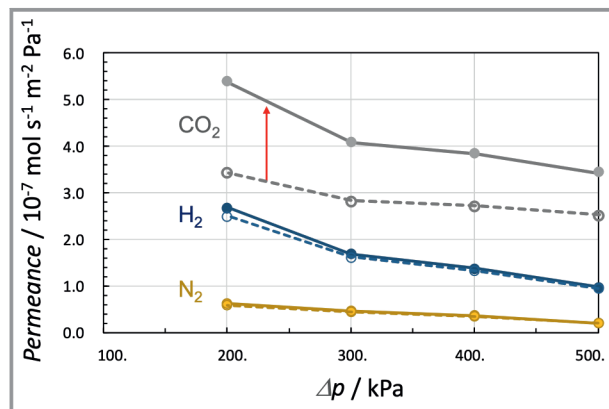


Figure 3. Example of correcting the observed permeance for the influence of the support for the single component permeation of CO_2 , N_2 , and H_2 through an SSZ-13 membrane at 295 K and different feed pressures. Permeate side at 100 kPa, no sweep gas used. Dashed lines observed permeance, solid lines corrected permeance over zeolite layer. Independently determined support parameters ($\epsilon/\tau = 0.35$, $d_0 = 2.0 \text{ mm}$, $\delta = 80 \text{ nm}$, $B_0^{\text{eff}} = 9.16 \times 10^{-17} \text{ m}^2$).

3 Examples

3.1 Operation Mode

Three different operation modes were used to study the single component permeation flux of propane through a silicalite-1 membrane. The zeolite was supported on a 3 mm thick porous stainless steel support [22]:

1. Feeding propane at the zeolite side and using helium as sweep gas at the permeate (support) side, 'WK-feed'.
2. Feeding propane at the support side and using helium as sweep gas at the zeolite (permeate) side, 'WK-perm'.
3. Propane is fed batchwise to a volume at the zeolite side and vacuum is pulled at the permeate side, determining the flux from the rate of pressure decrease, 'Batch'.

As a function of temperature, a flux maximum appears in all cases (Fig. 4), indicating a higher heat of adsorption ($-\Delta H_{\text{ads}}$) than the diffusion activation energy $E_{\text{a,diff}}$ [42]. This maximum was the highest and at the lowest temperature for the Batch mode. In this mode the propane pressure at the downstream side was the lowest, while the highest in the WK-feed mode. The fluxes decreased in the same order, Batch > WK-perm > WK-feed. The support resistance resulted in different local pressure at the zeolite layer surfaces, schematically presented in Fig. 2, yielding different propane gradients over the membrane and, hence different fluxes.

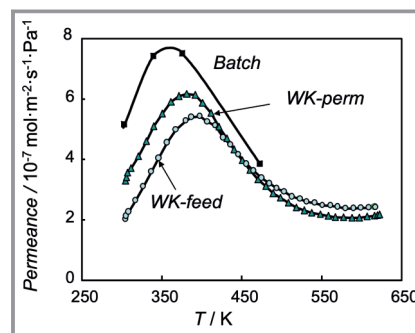


Figure 4. Effect of operation mode of the membrane on the permeance of propane through silicalite-1 as a function of the temperature at a feed pressure of 101 kPa. In the Wicke-Kallenbach (WK) experiments helium sweep gas was used, with both sides at 101 kPa, in the 'Batch' experiment vacuum was pulled at the permeate side. Reprinted with permission from [22]. Copyright Elsevier (1998).

3.2 Orientation of Membrane

The zeolite layer of the asymmetric composite membrane could face the feed side or the permeate side, which can have a big impact on the separation performance. This is illustrated for a mixture of methane and ethane of different composition and using helium as sweep gas with both sides at 101 kPa (Fig. 5) [21]. The silicalite-1 was supported by a 3 mm thick, porous stainless-steel disk. In the 'WK-feed' operation a composition dependent ethane selectivity of 6–10 was observed, while by reversing the orientation the selectivity was completely lost. In the 'WK-perm' mode the support acts as a stagnant gas layer, and due to the selective permeation of ethane concentration polarization occurs. As a result, the composition at the support-zeolite interface is enriched in methane, which counteracts the selectivity of the silicalite-1 selective layer. In Fig. 5b the local concentrations and selectivities are indicated for a 1:1 mixture of methane-ethane.

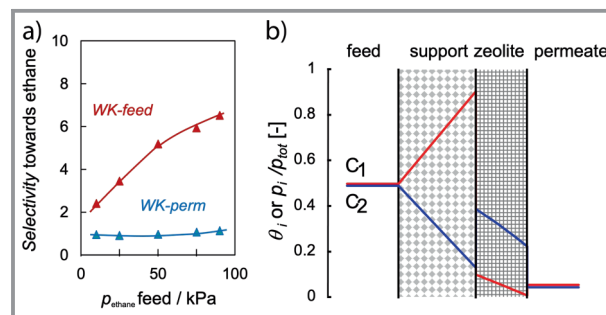


Figure 5. a) Selectivity for ethane in the permeation at 303 K of a mixture methane-ethane of different composition through a silicalite-1 membrane for two orientations: one with the silicalite-1 layer facing the feed side (WK-feed) and the support facing the permeate side, the other the reversed ('WK-perm'). b) Local concentrations in the membrane and selectivities of the layers for a 1:1 feed mixture in the 'WK-perm' configuration. In all cases helium is used as sweep gas at 101 kPa pressure at both sides. Reprinted with permission from [21]. Copyright 1998 ACS.

3.3 Support Thickness

The permeation behavior of a silicalite-1 membrane for a 95:5 methane/propane feed mixture as a function of the support thickness was modelled using the full GMS model for zeolite membranes and analogous GMS models for Knudsen and molecular diffusion with helium sweep [23]. The 'WK-feed' configuration described above was used in this analysis. The final fluxes were obtained from the transient solution evolution towards a steady state. The chambers at both sides of the membrane (101 kPa) were modelled as CSTRs to provide the boundary conditions for the simulation [37].

Fig. 6 presents the component fluxes, propane selectivity and component zeolite occupancies at the feed side and membrane-support interface. The thicknesses of two sup-

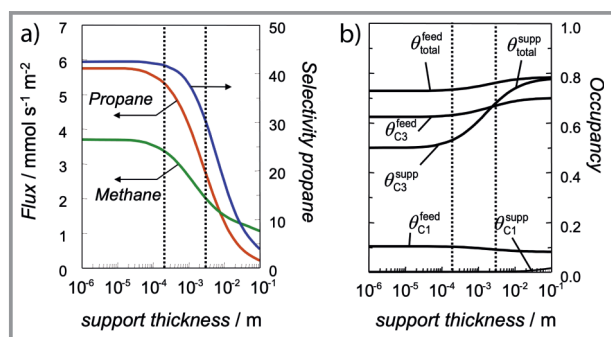


Figure 6. Simulation of the permeation of a 95:5 methane/propane mixture through a silicalite-1 membrane at 303 K according to the full GMS model as a function of the thickness of the support [37]. WK-method with helium sweep gas and silicalite-1 layer facing feed mixture, both sides 101 kPa. a) Fluxes of both components and selectivity for propane, b) the methane, propane, and total occupancy at the feed side and at the silicalite-1-support interface. Dashed lines indicate the thickness of used supports (a) Trumem, b) conventional porous sintered stainless steel sample). Reprinted with permission from [23]. Copyright 2005 Taylor and Francis.

ports used for the membranes studied are indicated – one was 3 mm [21] and the other was 0.4 mm (Trumem) [43].

The influence of the support thickness on the flux and permeation selectivity is clear: the thicker the support, the lower the fluxes and the poorer the selectivity for propane. For unrealistically thick supports the selectivity even reverses. This selectivity reversal occurs because the support performance dominates the membrane behavior and methane diffuses faster in helium than propane does. Also in the zeolite the entrainment effect of the tardier propane by the faster methane, intrinsic in the GMS model [44, 45], results in a higher local propane concentration at the zeolite-support interface, but also reduces the flux of propane through the membrane.

For the modelled conditions, the Trumem supported membrane is clearly superior, both concerning flux and selectivity. The Trumem support essentially did not impact the membrane performance. This example illustrates that the membrane performance (flux, selectivity) may be strongly affected by the support thickness. A silicalite-1 membrane layer supported on one support may behave completely differently from the same silicalite-1 membrane layer on a different support.

3.4 High-Flux Support

Fig. 7 is based on the room temperature single component permeation data of CO₂ for a two-layer supported high-flux all-silica CHA membrane without using a sweep gas [19]. For this system both support layers contribute to the pressure drop by viscous flow and Knudsen diffusion, with contributions of 25–40 % of the total pressure drop. Hence, the reported permeance for the membrane should be significantly corrected for this, yielding unrivalled permeances for this membrane.

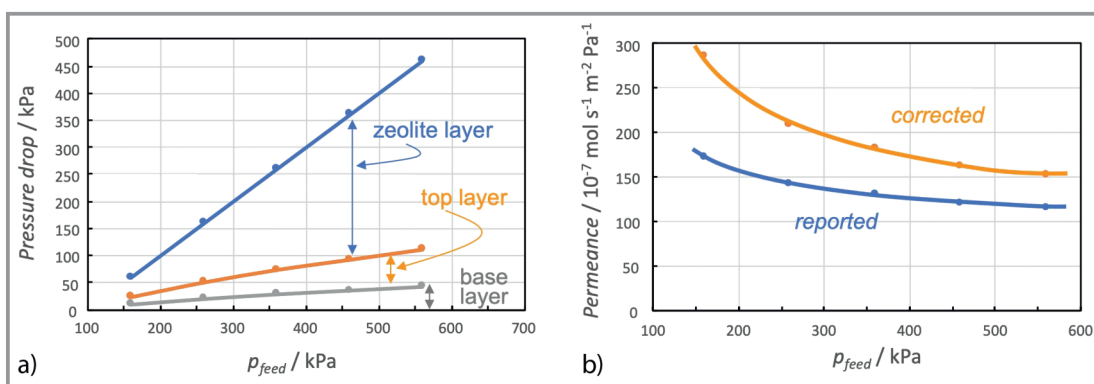


Figure 7. a) Pressure drop calculation for CO₂ permeation at 293 K at various feed pressures through a Si-CHA membrane on a two-layer alumina support. Permeate side 10⁵ Pa. b) Reported permeances and corresponding ones corrected for the pressure drop over the support layers. Data taken from [19]. Parameters used: (ϵ/τ) = 0.35 (assumed); base layer δ = 3.0 mm, d_0 = 3.0 μ m, D_{Kn}^{eff} = 1.31 $\times 10^{-4}$ m²s⁻¹, B_o^{eff} = 9.84 $\times 10^{-14}$ m², top layer δ = 30 μ m, d_0 = 100 nm, D_{Kn}^{eff} = 4.38 $\times 10^{-6}$ m²s⁻¹, B_o^{eff} = 1.09 $\times 10^{-16}$ m².

3.5 Membrane Characterization

As described earlier in the chapter, the permeance pressure dependence of permanent or weakly adsorbing gases can be used as fingerprint to detect whether or not a continuous zeolite layer has been formed on the support. In case large defects are present, viscous flow will take place, and the permeance will increase with increasing absolute pressure (see Eq. (14)). The flux through some zeolite membranes, however, can be so high that the resistance in the support can contribute to or dominate the transport characteristics of the membrane. As a result, the composite membrane can exhibit viscous flow characteristics even though the zeolite layer is continuous. This is demonstrated in Fig. 8 for ethane permeation at elevated temperature (weak adsorption) through a silicalite-1 membrane on a thin titania coated (15 μm) stainless steel support (0.4 mm) [24, 46]. After correction the permeance through the zeolite layer is constant, as expected according to Eq. (3).

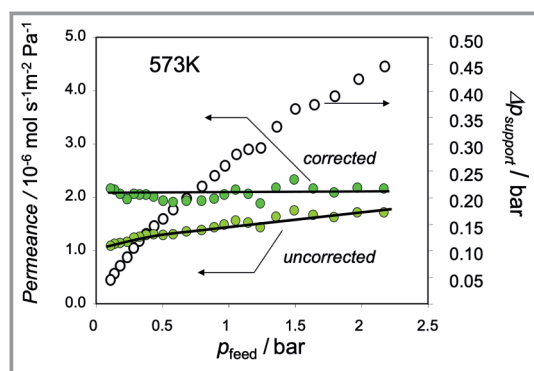


Figure 8. Permeance of ethane through a silicalite-1 membrane on Trumem support as a function of the ethane feed pressure at 573 K. Permeate side kept at vacuum. The top data are corrected for the effect of the viscous flow and Knudsen transport through the support, and reflect the permeance for the silicalite-1 layer only. Included is the calculated pressure drop over the support for the observed flux levels. Reprinted with permission from [23]. Copyright 2005 Taylor and Francis.

Therefore, an increasing permeance with increasing pressure does not necessarily indicate that the membrane possesses large defects in the zeolite layer.

3.6 Pervaporation

De Bruijn et al. analyzed numerous literature results on pervaporation of aqueous-organics mixtures through ceramic membrane systems, all consisting of a selective layer (silica or zeolite) on a support [25]. Generally, the selective layer was facing the liquid feed and the permeate side was kept at reduced pressure. Usually, a high selectivity is obtained in the dewatering applications, and the transport can be considered as a single component diffusion through the membrane. For the zeolite membranes (A-type or T-type) high

occupancies can be expected at the lower temperatures due to their high hydrophilicity.

As outlined above by including the Knudsen and viscous transport over the support, the authors calculated the partial pressures of the permeating components at the zeolite-support interface and compared those with the 'virtual' pressures corresponding to the feed side conditions of temperature and liquid composition. This yielded the contribution of the support in the overall pressure drop over the membrane.

In several cases the major or complete pressure drop was over the support, indicating that this constitutes a major resistance (Fig. 9) [25]. The highest fluxes (up to 30 $\text{kg H}_2\text{O m}^{-2}\text{h}^{-1}$) were obtained for the thinnest and supports of high porosity. Although in these cases the support resistance, expressed as relative pressure drop, was moderate ($\sim 29\%$), in absolute value it is the largest. Clearly, especially in water removal applications the fluxes could be increased by using thinner and more porous supports.

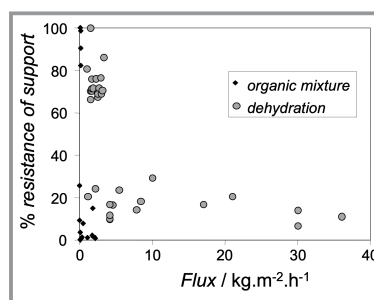


Figure 9. % Resistance of support versus flux in pervaporation literature of water-organics and of organic-organic mixture separation by microporous ceramic (including zeolitic) membranes. Reprinted with permission from [25]. Copyright Elsevier (2003).

4 Concluding Remarks

The development of supported membranes for real life applications covers aspects from selective material identification through manufacturing to process integration [47, 48]. The examples given above show the importance of a correctly applied composite zeolite membrane with an optimized design of the zeolite support layer, in order to optimally utilize the intrinsic separation selectivity of the zeolite layer and to maximize the productivity of the membrane. Also, disregarding a support correction in modeling transport studies wrong conclusions can be expected. Apparent permeance levels above $\sim 5 \times 10^{-7} \text{ mol s}^{-1} \text{ m}^{-2} \text{ Pa}^{-1}$ deserve more detailed analysis.

A support often consists of a coarse layer to reduce the transport resistance with a finer top layer in order to avoid defect formation in the zeolite layer manufacturing. The transport resistance of the support should be minimized to maximize the flux and selectivity, as the (Knudsen) separation characteristics are counteracting the zeolite selectivity.

This can be achieved by a low thickness, large pore material, although this makes the zeolite layer synthesis more challenging. The contribution of the support can be quantified by application of the Dusty gas model, including the transport contributions of Knudsen and molecular diffusion and viscous flow [39, 40].

In a zeolite membrane the zeolite layer should always be oriented towards the feed side, as otherwise a strong concentration polarization will develop in the stagnant gas layer in the support, also counteracting the zeolite selectivity and lowering the productivity.

The development of high-flux membranes by thin support and thin zeolite layers puts questions on the validity of the assumption of adsorption equilibrium at both sides and zeolite diffusion as rate determining process to model the transport through the zeolite layer, and modeling relations should be reconsidered for these systems [49, 50]. Entering or leaving the zeolite layer may become rate determining as well, e.g., [33, 35]. Further, in the examples given concentration polarization in the fluid phase were disregarded but may become important as well in high-flux membrane modules. A proper design with inserts can minimize this influence.

No attention has been paid to the membrane synthesis, but apart from reaching a continuous layer, the orientation of the zeolite layer with a 1D or 2D pore structure becomes important for the performance [51–53], which applies to MOF membranes as well [54–57].

In retrospect, these findings suggest preference for the use of two configuration modules:

- a module based on a bundle of thin hollow fiber supports with the zeolite layer at the fiber outside [58].
- a monolithic module with alternating channel layers for feed and permeate, with the zeolite layer at the feed side of the thin channel walls [59].

Multichannel (4–36 channels) rods with zeolite coated channel walls are less preferred since the diffusion distance to the rod outside (permeate) in such support will vary strongly for different channels and is on average quite long.

Next to the cost of manufacturing, a choice for one of these options will further depend on the ease of zeolite synthesis, mechanical robustness of the unit and company expertise.

XW acknowledges National Natural Science Foundation of China (21908097), Jiangsu Specially-Appointed Professors Program

Symbols used

B_0	[m ²]	permeability in viscous flow
d_0	[m]	pore diameter
D	[m ² s ⁻¹]	transport diffusivity
D_i	[m ² s ⁻¹]	Maxwell Stefan diffusivity of component i in zeolite

D_{ij}	[m ² s ⁻¹]	Maxwell Stefan exchange diffusivity between component i and j
E_a	[kJ mol ⁻¹]	activation energy
ΔH	[kJ mol ⁻¹]	enthalpy of adsorption
K	[Pa ⁻¹]	adsorption equilibrium constant
M	[kg mol ⁻¹]	molar mass
N	[mol s ⁻¹ m ⁻²]	molar flux
p	[Pa]	pressure
q	[mol kg ⁻¹]	loading in zeolite
R	[J mol ⁻¹ K ⁻¹]	gas constant
S_{ij}	[–]	selectivity of component i over j
T	[K]	temperature
y	[–]	molar fraction in gas phase

Greek letters

Γ	[–]	Thermodynamic correction factor
δ	[m]	Membrane thickness
Δ	[–]	Difference
ε	[–]	Porosity
η	[Pa s]	Viscosity
Π	[mol s ⁻¹ m ⁻² Pa ⁻¹]	Permeance
θ	[–]	Fractional occupancy in zeolite
ρ	[kg m ⁻³]	Density zeolite
τ	[–]	Tortuosity
∇	[m ⁻¹]	Gradient

Sub- and superscripts

ads	adsorption
diff	diffusion
eff	effective
i, j	components i, j
Kn	Knudsen
perm	permeate
sat	saturation
sup	support
visc	Viscous
0	inlet side membrane, initial
δ	outlet, permeate side membrane

References

- [1] M. Noack, P. Kölsch, R. Schäfer, P. Toussaint, J. Caro, *Chem. Ing. Tech.* **2001**, 73 (8), 958–967.
- [2] J. Caro, M. Noack, P. Kölsch, H. Schellevis, R. Schäfer, *Microporous Mesoporous Mater.* **2000**, 38, 3–24.
- [3] J. Caro, M. Noack, *Microporous Mesoporous Mater.* **2008**, 115 (3), 215–233.
- [4] M. Noack, P. Kölsch, J. Caro, M. Schneider, P. Toussaint, I. Sieber, *Microporous Mesoporous Mater.* **2000**, 35–36, 253–265.
- [5] D. Shah, K. Kissick, A. Ghorpade, R. Hannah, D. Bhattacharyya, *J. Membr. Sci.* **2000**, 179 (1–2), 185–205.

- [6] Y. Morigami, M. Kondo, J. Abe, H. Kita, K. Okamoto, *Sep. Purif. Technol.* **2001**, 25 (1–3), 251–260.
- [7] K. Sato, K. Sugimoto, N. Shimotsuma, T. Kikuchi, T. Kyotani, T. Kurata, *J. Membr. Sci.* **2012**, 409, 82–95.
- [8] K. Sato, K. Sugimoto, T. Nakane, *J. Membr. Sci.* **2008**, 310 (1–2), 161–173.
- [9] K. Sato, K. Sugimoto, T. Nakane, *J. Membr. Sci.* **2008**, 319 (1–2), 244–255.
- [10] A. Urtiaga, E. D. Gorri, C. Casado, I. Ortiz, *Sep. Purif. Technol.* **2003**, 32 (1–3), 207–213.
- [11] S. G. Li, V. A. Tuan, R. D. Noble, J. L. Falconer, *Ind. Eng. Chem. Res.* **2001**, 40 (21), 4577–4585.
- [12] H. Kita, K. Horii, Y. Ohtoshi, K. Tanaka, K. I. Okamoto, *J. Mater. Sci. Lett.* **1995**, 14, 206–208.
- [13] J. F. Smetana, J. L. Falconer, R. D. Noble, *J. Membr. Sci.* **1996**, 114, 127–130.
- [14] X. S. Chen, X. Lin, P. Chen, H. Kita, *Desalination* **2008**, 234 (1–3), 286–292.
- [15] J. Kuhn, K. Yajima, T. Tomita, J. Gross, F. Kapteijn, *J. Membr. Sci.* **2008**, 321 (2), 344–349.
- [16] L. Sandström, E. Sjöberg, J. Hedlund, *J. Membr. Sci.* **2011**, 380 (1–2), 232–240. DOI: <https://doi.org/10.1016/j.memsci.2011.07.011>
- [17] D. Korelskiy, T. Leppajarvi, H. Zhou, M. Grahn, J. Tanskanen, J. Hedlund, *J. Membr. Sci.* **2013**, 427, 381–389. DOI: <https://doi.org/10.1016/j.memsci.2012.10.016>
- [18] S. Karimi, D. Korelskiy, L. Yu, J. Mouzon, A. A. Khodadadi, Y. Mortazavi, M. Esmaeili, J. Hedlund, *J. Membr. Sci.* **2015**, 489, 270–274. DOI: <https://doi.org/10.1016/j.memsci.2015.04.038>
- [19] L. Yu, A. Holmgren, M. Zhou, J. Hedlund, *J. Mater. Chem. A* **2018**, 6 (16), 6847–6853. DOI: <https://doi.org/10.1039/c8ta01240g>
- [20] L. Yu, D. Korelskiy, M. Grahn, J. Hedlund, *Sep. Purif. Technol.* **2015**, 153, 138–145. DOI: <https://doi.org/10.1016/j.seppur.2015.09.005>
- [21] J. M. v. d. Graaf, E. v. d. Bijl, A. Stol, F. Kapteijn, J. A. Moulijn, *Ind. Eng. Chem. Res.* **1998**, 37 (10), 4071–4083.
- [22] J. M. v. d. Graaf, F. Kapteijn, J. A. Moulijn, *J. Membr. Sci.* **1998**, 144, 87–104.
- [23] F. Kapteijn, W. Zhu, J. A. Moulijn, T. Q. Gardner, in *Structured catalysts and reactors*, 2nd ed. (Eds: A. Cybulski, J. A. Moulijn), CRC Press, Boca Raton, FL **2006**.
- [24] N. Nishyama, L. Gora, V. V. Tepliyakov, F. Kapteijn, J. A. Moulijn, *Sep. Purif. Technol.* **2001**, 22–23, 295–307.
- [25] F. T. d. Bruijn, Z. Olujic, P. J. Jansens, F. Kapteijn, *J. Membr. Sci.* **2003**, 223, 141–156.
- [26] J. v. d. Bergh, W. Zhu, J. Gascon, J. A. Moulijn, F. Kapteijn, *J. Membr. Sci.* **2008**, 316 (1–2), 35–45.
- [27] J. v. d. Bergh, A. Tihaya, F. Kapteijn, *Microporous Mesoporous Mater.* **2010**, 132 (1–2), 137–147.
- [28] H. van Koningsveld, J. C. Jansen, *Acta Crystallogr. Sect. A Found. Adv.* **1996**, 52, C403. DOI: <https://doi.org/10.1107/S0108767396083389>
- [29] M. Yu, T. J. Amundsen, M. Hong, J. L. Falconer, R. D. Noble, *J. Membr. Sci.* **2007**, 298 (1–2), 182–189.
- [30] X. R. Wang, Y. T. Zhang, X. Y. Wang, E. Andres-Garcia, P. Du, L. Giordano, L. Wang, Z. Hong, X. H. Gu, S. Murad, F. Kapteijn, *Angew. Chem. Int. Ed.* **2019**, 58 (43), 15518–15525. DOI: <https://doi.org/10.1002/anie.201909544>
- [31] P. J. Bereciartua, Á. Cantín, A. Corma, J. L. Jordá, M. Palomino, F. Rey, S. Valencia, E. W. Corcoran, P. Kortunov, P. I. Ravikovitch, A. Burton, C. Yoon, Y. Wang, C. Paur, J. Guzman, A. R. Bishop, G. L. Casty, *Science* **2017**, 358 (6366), 1068. DOI: <https://doi.org/10.1126/science.aao0092>
- [32] D. M. Ruthven, J. Kärger, S. Brandani, E. Mangano, *Adsorption* **2021**, 27 (5), 787–799. DOI: <https://doi.org/10.1007/s10450-020-00257-w>
- [33] G. Sastre, J. Kärger, D. M. Ruthven, *Adsorption* **2021**, 27 (5), 777–785. DOI: <https://doi.org/10.1007/s10450-020-00260-1>
- [34] R. M. Barrer, *J. Chem. Soc. Faraday Trans.* **1992**, 88 (10), 1463–1471.
- [35] R. M. Barrer, *J. Chem. Soc., Faraday Trans.* **1990**, 86 (7), 1123–1130.
- [36] F. Kapteijn, W. J. W. Bakker, J. M. v. d. Graaf, G. Zheng, J. Poppe, J. A. Moulijn, *Catal. Today* **1995**, 25, 213–218.
- [37] J. M. v. d. Graaf, F. Kapteijn, J. A. Moulijn, *AIChE J.* **1999**, 45 (3), 497–511.
- [38] F. Kapteijn, J. A. Moulijn, R. Krishna, *Chem. Eng. Sci.* **2000**, 55, 2923–2930.
- [39] S. Thomas, R. Schäfer, J. Caro, A. Seidel-Morgenstern, *Catal. Today* **2001**, 67 (1), 205–216. DOI: [https://doi.org/10.1016/S0920-5861\(01\)00288-7](https://doi.org/10.1016/S0920-5861(01)00288-7)
- [40] R. Krishna, *Gas Sep. Purif.* **1993**, 7 (2), 91–104.
- [41] J. Caro, *Adsorption* **2021**, 27 (3), 283–293. DOI: <https://doi.org/10.1007/s10450-020-00262-z>
- [42] F. Kapteijn, J. M. v. d. Graaf, J. A. Moulijn, *AIChE J.* **2000**, 46 (5), 1096–1100.
- [43] L. Trusov, *Membr. Technol.* **2000**, 2000 (128), 10–14.
- [44] R. Krishna, S. Li, J. M. van Baten, J. L. Falconer, R. D. Noble, *Sep. Purif. Technol.* **2008**, 60 (3), 230–236.
- [45] R. Krishna, *Chem. Soc. Rev.* **2012**, 41 (8), 3099–3118.
- [46] L. Gora, N. Nishyama, J. C. Jansen, F. Kapteijn, V. V. Tepliyakov, T. Maschmeyer, *Sep. Purif. Technol.* **2001**, 22–23, 223–229.
- [47] S. P. Nunes, P. Z. Culfaz-Emecen, G. Z. Ramon, T. Visser, G. H. Koops, W. Jin, M. Ulbricht, *J. Membr. Sci.* **2020**, 598, 117761. DOI: <https://doi.org/10.1016/j.memsci.2019.117761>
- [48] U. Beuscher, E. J. Kappert, J. G. Wijmans, *J. Membr. Sci.* **2022**, 643, 119902. DOI: <https://doi.org/10.1016/j.memsci.2021.119902>
- [49] P. Kumar, D. W. Kim, N. Rangnekar, H. Xu, E. O. Fetisov, S. Ghosh, H. Zhang, Q. Xiao, M. Shete, J. I. Siepmann, T. Dumitrica, B. McCool, M. Tsapatsis, K. A. Mkhoyan, *Nat Mater* **2020**, 19 (4), 443–449. DOI: <https://doi.org/10.1038/s41563-019-0581-3>
- [50] J. Caro, J. Kärger, *Nat Mater* **2020**, 19 (4), 374–375. DOI: <https://doi.org/10.1038/s41563-020-0630-y>
- [51] M. Noack, P. Kölsch, D. Venzke, P. Toussaint, J. Caro, *Microporous Mater.* **1994**, 3, 201–206.
- [52] K. V. Agrawal, B. Topuz, P. Tung Cao Thanh, N. Thanh Huu, N. Sauer, N. Rangnekar, H. Zhang, K. Narasimharao, S. N. Basahel, L. F. Francis, C. W. Macosko, S. Al-Thabaiti, M. Tsapatsis, K. B. Yoon, *Adv. Mater.* **2015**, 27 (21), 3243–3249. DOI: <https://doi.org/10.1002/adma.201405893>
- [53] J. S. Lee, K. Ha, Y. J. Lee, K. B. Yoon, *Adv. Mater.* **2005**, 17 (7), 837–841.
- [54] J. Caro, *Chem. Ing. Tech.* **2018**, 90 (11), 1759–1768. DOI: <https://doi.org/10.1002/cite.201800034>
- [55] Q. H. Qian, P. A. Asinger, M. J. Lee, G. Han, K. M. Rodriguez, S. Lin, F. M. Benedetti, A. X. Wu, W. S. Chi, Z. P. Smith, *Chem. Rev.* **2020**, 120 (16), 8161–8266. DOI: <https://doi.org/10.1021/acs.chemrev.0c00119>
- [56] Y. S. Li, H. Bux, A. Feldhoff, G. L. Li, W. S. Yang, J. Caro, *Adv. Mater.* **2010**, 22 (30), 3322–3326.
- [57] J. Gascon, F. Kapteijn, *Angew. Chem. Int. Ed.* **2010**, 49 (9), 1530–1532.
- [58] Y. M. Liu, X. R. Wang, Y. T. Zhang, Y. He, X. H. Gu, *Chin. J. Chem. Eng.* **2015**, 23 (7), 1114–1122. DOI: <https://doi.org/10.1016/j.cjche.2015.04.006>
- [59] J. Okazaki, H. Hasegawa, N. Chikamatsu, K. Yajima, K. Shimizu, M. Niino, *Sep. Purif. Technol.* **2019**, 218, 200–205. DOI: <https://doi.org/10.1016/j.seppur.2019.02.049>